SCIENCE CHINA
Technological Sciences

• Article •

April 2014 Vol.57 No.4: 811–818
doi: 10.1007/s11431-014-5486-4

Pressure fluctuation propagation of a pump turbine at pump mode under low head condition

GUO Lei[1], LIU JinTao[2], WANG LeQin[1*], QIN DaQing[3] & WEI XianZhu[3]

[1] *Institute of Process Equipment, Zhejiang University, Hangzhou 310027, China;*
[2] *Beijing Institute of Control Engineering, China Aerospace Science and Technology Corporation, Beijing 100190, China;*
[3] *State Key Laboratory of Hydropower Equipment, Harbin 150001, China*

Received October 21, 2013; accepted December 18, 2013

Pressure fluctuation at the vaneless space and vanes passages is one of the most important problems for the stable operation of a pump turbine. The fluctuation appears in any operating condition. Much research has been done on the pressure fluctuation of hydraulic machinery. However, the details of pressure fluctuation propagation of the pump turbine at the pump mode have not been revealed. The modern pump turbine with high water head requires the runner to be "flat", which would induce pressure fluctuation more easily than the low head pump turbine. In this article, a high head pump turbine model is used as the research object. As the pressure fluctuation at off-design point is more serious than at the design point, the low head condition is chosen as the research condition. Pressure fluctuation at the vaneless space and vanes passages is predicted by the computational fluid dynamics method based on k-ω shear stress transport model. The experiment conducted on the test rig of the Harbin Institute of Large Electrical Machinery is used to verify the simulation method. It proves that the numerical method is a feasible way to research the fluctuation under this operating condition. The pressure fluctuation along the passage direction is analyzed at time and frequency domains. It is affected mainly by the interaction between the runner and vanes. In the circumferential direction, the influence of the special stay vane on the pressure fluctuation is got. The amplitude in the high-pressure side passage of that vane is lower than that in the other side. The study provides a basic understanding of the pressure fluctuation of a pump turbine and could be used as a reference to improve the operation stability of it.

pump turbine, pressure fluctuation, vaneless space, vanes passage, pump mode, low head

Citation: Guo L, Liu J T, Wang L Q, et al. Pressure fluctuation propagation of a pump turbine at pump mode under low head condition. Sci China Tech Sci, 2014, 57: 811–818, doi: 10.1007/s11431-014-5486-4

1 Introduction

Pumped storage plant (PSP) is widely used as a kind of reliable power source for the electric grid regulation. With the increasing installed capacity, the stability of the PSP becomes very important for the security of the electric system. Since pump turbine is the key equipment of the PSP, its stability attracts increasing attention. Pressure fluctuations, vibrations, and swings are three major unfavorable phenomena to deteriorate the stability of hydraulic turbine systems [1]. The fast and frequent switching between pumping and generating modes as well as extended operations at off-design conditions pose technical challenges for the pump turbine [2]. The pressure fluctuation induced by the complex inner flow exists in nearly any operation condition. At the same time, the pressure fluctuation is a main resource of mechanical vibration and fatigue. For these reasons, pressure fluctuation is an important indicator to evaluate the security level in the final test of the pump turbine.

*Corresponding author (email: hj_wlq2@zju.edu.cn)

The pressure fluctuation problems have been studied for about 40 years. Experiment is a traditional and effective method for hydraulic machinery [2–5]. For the generating mode of the pump turbine, Husmatuchi and Farhat [2] tested the pressure fluctuation under off-design operating conditions with the help of 30 pressure sensors (but only three sensors in one vane passage). For the pump mode of the pump turbine, Ran et al. [3] did a research about the pressure fluctuation on the model test rig, and five transducers were set in this test.

Nevertheless, the experiment is limited by the time and cost. Also, the experimental method has other limitations. For example, in a normal test, it is difficult to obtain the inner flow information, and usually, only a small number of transducers were available. In general, the experiment method may not provide enough data for the research of pressure fluctuation propagation.

With the development of computer technology, complex flows in the whole passage of the hydraulic turbines could be analyzed by the computational fluid dynamics (CFD) method since the end of the 1990s [1]. Without doubt, the experiment provides the most reliable and convincing results to verify the numerical method.

Pressure fluctuations in different kinds of hydraulic machinery have been studied. For turbines, Chen and Li [6] numerically investigated the guide-plate induced pressure fluctuations on guide vanes of three gorges turbines. Xiao et al. [7] discussed the pressure pulses characteristics in a Francis turbine by experimental and numerical methods. The simulation results displayed unsteady flow patterns. Since more monitoring points were set in the simulation than in the experiment, fluctuation details at a partial load were revealed. The works of Wang et al. [8] focused on the pressure fluctuation of a large Francis turbine's runner. Gong et al. [9] has simulated the pressure fluctuation in a 1000 MW Francis turbine under small opening conditions with DES method. Qian et al. [10] researched the influence of misaligned guide vanes on the pressure fluctuation in a Francis turbine. Rivetti et al. [11] simulated the pressure fluctuation in a prototype Kaplan turbine. Liu et al. [12] and Wu et al. [13] predicted the pressure fluctuation of the model and prototype Kaplan turbine by unsteady turbulent flow simulation. Yang et al. [14] researched the influence of the blade number on the performance and pressure fluctuation in a pump when used as a turbine.

For pump turbine, Zobeiri et al. [15] has studied the pressure fluctuation in the distributor channels induced by rotor-stator interactions in the generating mode. Xiao et al. [16], Liu et al. [17], and Sun et al. [18] studied the pressure fluctuation of the pump turbine with misaligned guide vanes.

Researches above focus on the turbine mode. For the pump operation, ref. [3] did a series of experiments. Sun et al. [19] studied the pressure fluctuation in different guide vanes' opening angle at pump mode. Spence and Joao [20] investigated a centrifugal pump by CFD. Shi and Tsukamoto [21] researched the impeller-interaction caused pressure fluctuation in a diffuser pump stage. Then Wang and Tsukamoto [22] investigated the unsteady flow in it under off-design condition by both experimental and numerical methods. The structure situations of the pump in those two articles are similar to the pump turbine at the pump mode.

However, the works done before have not given the propagation details of the fluctuation in the vaneless space and vanes passages. Compared with the normal turbine, the pump turbine has the unique pump mode. On the other hand, considering the requirement of the turbine mode, its pump characteristics are different from the traditional pump. The pressure fluctuation is investigated a lot for the traditional turbine and pump, but for the pump mode of the pump turbine, the relative research is not enough, especially at the off-design points, such as the low head condition. As this condition is far from the design point, pressure fluctuation would be more serious than in the design condition.

In this article, a high head pump turbine was chosen as the object. The propagation law of pressure fluctuation under the off-design low head condition was revealed. The geometry of pump turbine includes full flow passage. Vanes, blades and draft tube were discretized by high quality hexahedral meshes. Firstly, the numerical calculation was verified by the experimental data. Then, the pressure fluctuation data were transformed by the fast Fourier transform (FFT) method. Finally, the propagation law of pressure fluctuation at the time and frequency domains were analyzed.

2 Numerical models and computational schemes

2.1 Geometry and grid

The computational model includes the case, stay vanes, guide vanes, the runner, and the draft tube (Figure 1). The principal specifications of the pump turbine are listed in Table 1.

As the turbulence model requires high quality mesh, pump turbine components (except the case) has been discretized by hexahedral grids. Tetrahedral mesh was used at the case part.

To validate the independence of the grids, six sets of grids with different amount of elements were tested based on the water head. The results are given in Table 2. Finally,

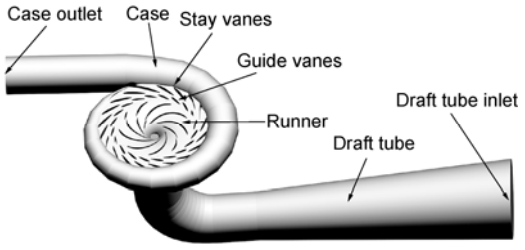

Figure 1 Hydraulic model of the pump turbine.

Table 1 Specifications of the pump turbine model

Parameters	Values
Runner inlet diameter in the pump mode (mm)	240
Runner outlet diameter in the pump mode (mm)	482.5
Blade number	9
Blade wrap angle (°)	105
Guide vane number	20
Height of vanes (mm)	42.25
Distribution diameter of guide vanes (mm)	563.5
Case wrap angle (°)	345
Case outlet diameter (mm)	260
Draft tube inlet diameter (mm)	545.5

Table 2 Grid independent study

	Total number of elements	Water head (m)
1	9910407	41.55
2	8162982	41.71
3	6584406	41.73
4	5104706	41.47
5	4173614	41.07
6	3321769	41.22

a mesh of 8.16 million elements and 6.64 million nodes was employed for the computational domain.

To reduce the y+ of the blades and vanes, local refinements were applied at those places. For guide vanes, the height of the first layer near the wall was 0.02 mm and the height ratio was 1.2. For stay vanes and blades, the height of the first layer was 0.05 mm and the height ratio was 1.5. Figure 2 shows the mesh assembly of the components.

Meshes of five computational domains were generated separately by the commercial software ICEM and the adjacent parts were connected by the interface in the CFD software. The mesh information is given in Table 3.

2.2 Turbulence model and boundary conditions

The k-ω based shear stress transport (SST) model designed by Menter [23] has been employed to close the governing equations. This model is devised by combining the good

Figure 2 Mesh of vanes and runner.

Table 3 Mesh information for each part

Components	Number of elements	Number of nodes
Case	1332913	235608
Stay vane	1721464	1585040
Guide vane	1692722	1549440
Runner	2194875	2075472
Draft tube	1221008	1196517
Total	8162982	6642077

near-wall behavior of the k-ω model with the k-ε model used away from the walls. The applications have verified its reliability. In refs. [7,8,16,18,19], the SST turbulence model was used. These articles showed that it was suitable to be applied in the pressure fluctuation research.

The commercial CFD code Fluent was employed to perform the simulation.

For the SST model, low-*Re* corrections were used. The other data was the default set in Fluent. The semi-implicit method for pressure-linked equations consistent (SIMPLEC) was used for the discretized equations. For the spatial discretization, second order was set for the pressure and second order upwind scheme was set for the momentum, turbulent kinetic energy, and dissipation rate. A second order implicit scheme was applied for time discretization.

A uniform velocity was used as the draft tube inlet boundary condition. Pressure outlet boundary condition was used at the downstream case outlet boundary. Intensity and hydraulic diameter was used in both of them for the specification method. For the inlet condition, turbulent intensity was 2% and hydraulic diameter was 545.5 mm. For the outlet condition, the backflow turbulent intensity was 4% and the backflow hydraulic diameter was 260 mm. The passage walls except the runner were all set to be no-slip condition. Steady state was simulated as the initial condition of the unsteady simulation. Steady simulation was set according to the test operation data.

Multiple rotating reference frames (MRF) method was used for the steady simulation, while the moving mesh method was used for the unsteady simulation.

In the unsteady simulation, the time step was set to be 0.0001388889 s. As the rotational speed is 1200 r/min, the time step is just the time that the runner takes to rotate by 1°. According to the sampling theorem, that time step can cover the frequencies that this article focuses on. The maximum iteration loop was set as 100 and the residual errors were set as 0.00001.

2.3 Monitoring points

To get the propagation law of the pressure fluctuation along the vanes passages and in the circumferential direction, 5 passages were set as the research objects and 10 monitoring points were set at each passage. The monitor scheme is shown in Figure 3.

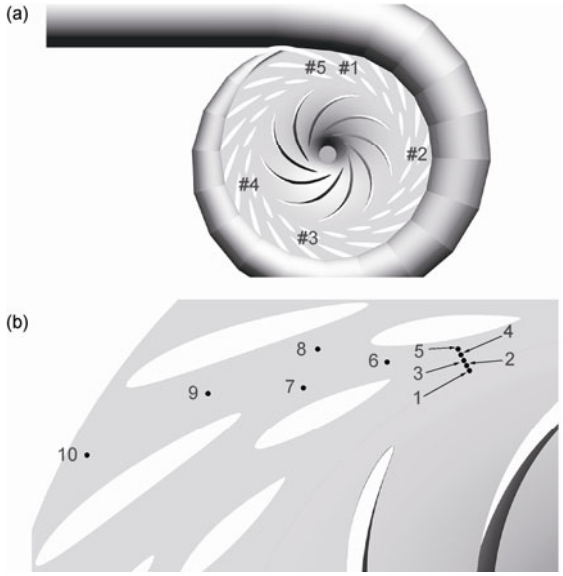

Figure 3 The monitoring points distribution. (a) Distribution of five object passages; (b) monitoring points in the object passages.

3 Results and discussion

3.1 Measurement of pressure fluctuation in the model machine and the validation of CFD

The pressure fluctuation experiment of this model pump turbine has been conducted on the test rig of the Harbin Institute of Large Electrical Machinery. The guide vanes opening is 16° and the rotational speed is 1200 r/m. The experimental conditions are listed in Table 4 where n_{11} is the unit speed, Q_{11} is the unit discharge, n is the rotating speed, Q is the discharge, and γ is the guide vane opening.

The comparison between the experimental data and the simulation results are listed in Table 5, in which, H is the water head and ΔH is the mixing peak-to-peak value of the pressure fluctuation. The results verified the method used in this article.

3.2 Pressure fluctuation propagation along the passage

In the vanes passages, the fluctuation spectrum changes with the distance to the runner. The pressure fluctuation changing trend along the passage is similar in different passages. This article takes passage 4 as an example. The pressure fluctuation at different time domains is presented in Figure 4.

At the pump mode, pump turbine works as a centrifugal pump. The water flows from the monitoring points 1 to 10. The average pressure near the outlet is higher than the other places. In Figure 4, it is clearly shown that the pressure increases from points 1 to 10. At the same time, Figure 4 shows that pressure fluctuations at the vaneless space and guide vane passage are obvious. At the stay vanes passage, that is points 8–10, the amplitude decreases quickly. For more information, it can be analyzed at the frequency domain as shown in Figure 5.

As shown in Figure 3, monitoring points 1–4 are at the vaneless space. At point 1, which is the nearest monitoring point to the runner, the influence of runner rotation is obvious. The first dominant frequency of this point is $9f_n$ (f_n is the rotational frequency of the runner and its value is 20 Hz), which is the blades passing frequency of the runner. The second dominant frequency is $18f_n$. Considering the number of guide vanes to be 20, this frequency is influenced by the runner and the vanes at the same time. The third dominant frequency is $27f_n$ followed by $36f_n$ and $4.5f_n$, which have low amplitudes. In this area, the rotor-stator interaction is the main reason for the fluctuation. Because of the requirement of the pump mode, pump turbine runner is lower than the normal turbine in the height direction. Also, the pump turbine develops towards the high water head, which will lead to the decreasing of the specific speed. It requires the runner to be "flat", and the thickness of the blades and vanes' outlet side to be bigger than the normal turbine. Therefore, the wake flow may induce serious nonuniform flow field and rotate with the runner by the force of water pressure. At the same time, the periodic potential flow disturbances interact with that wake flow. Therefore, the rotor-stator interaction of high head pump turbines is more serious than that in the normal turbine.

Table 4 Experimental conditions

n_{11} (r/min)	Q_{11} (L/s)	n (r/min)	Q (L/s)	γ (°)
45.916	742.554	1200	268.274	16

Table 5 Comparison between the experimental and CFD results

	H (m)	$\Delta H/H$ (%)
EXP	39.342	5.705
CFD	41.709	5.608
Diff.	6.017%	−1.710%

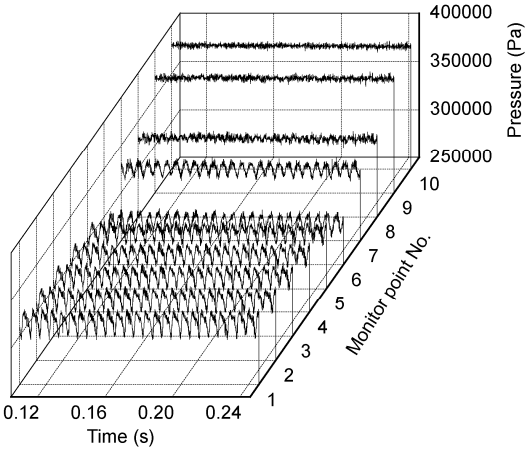

Figure 4 Pressure fluctuation of passage 4 at different time domains.

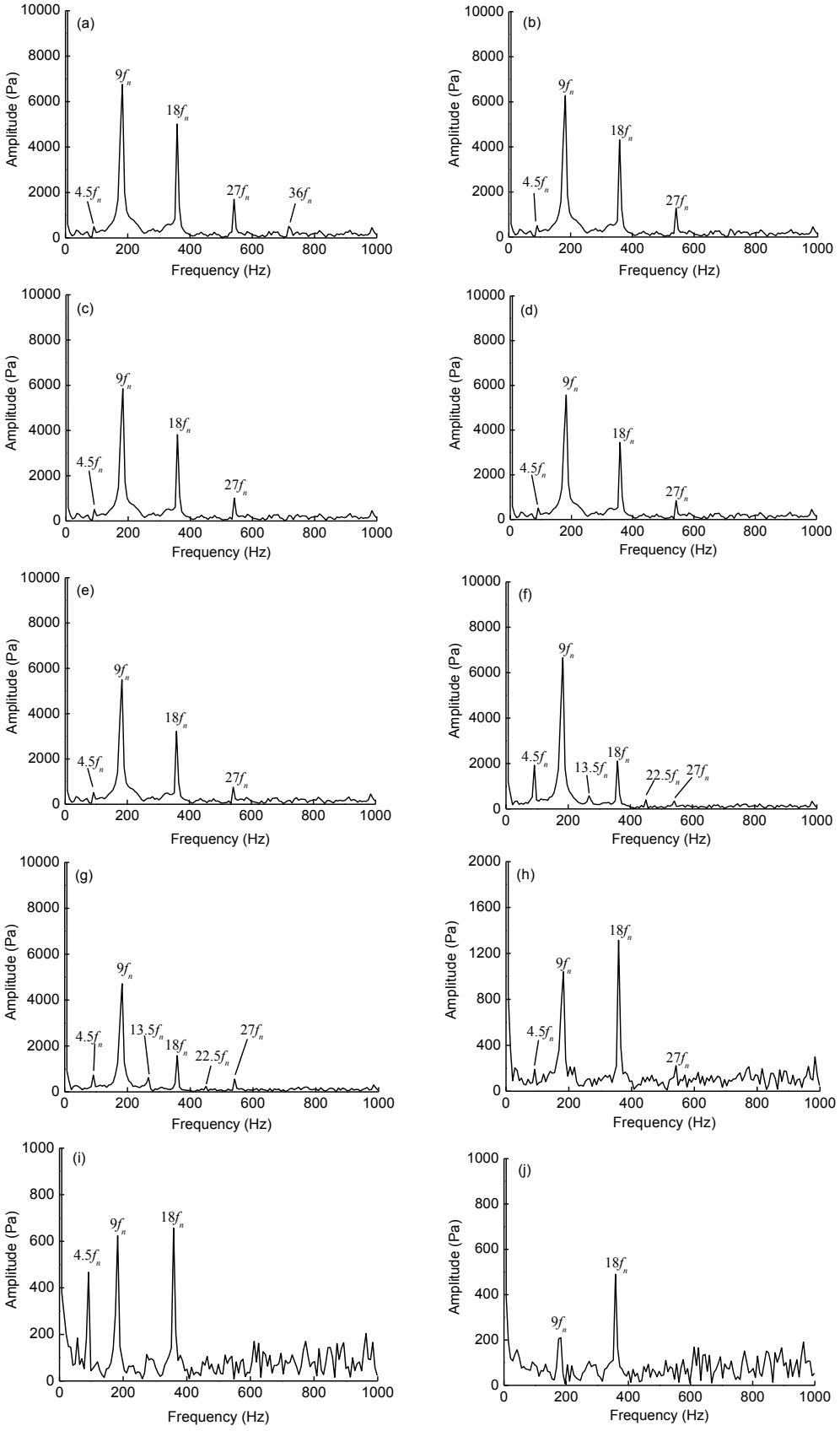

Figure 5 Pressure fluctuation of passage 4 at different frequency domains. (a) Monitoring point 1; (b) monitoring point 2; (c) monitoring point 3; (d) monitoring point 4; (e) monitoring point 5; (f) monitoring point 6; (g) monitoring point 7; (h) monitoring point 8; (i) monitoring point 9; (j) monitoring point 10.

The situations of points 2–4 are similar to point 1. There is not any other structure in this area and hence the reason for fluctuation is the same. Frequency distribution and the relationship between them are similar to point 1 at the time and frequency domains. The only variable is the distance between the monitoring point and the runner. With increasing distance, the influence of the rotation becomes small. Thus, the main difference is the amplitude. It decreases from point 1 to 4.

Point 5 is at the entrance of the guide vanes passage. The frequency components are similar to the vaneless space points and the amplitude of it is lower than those points. Along the flow direction, the next point is point 6. It is at the middle of the guide vanes passage. Because of the guide vanes, the frequency distribution is different with the vaneless space. $4.5f_n$ component increases obviously. The $13.5f_n$ and $22.5f_n$ become obvious. Those two frequency values just equal $4.5f_n$ plus passing frequency $9f_n$ and twice passing frequency $18f_n$. At point 4, that is the exit of guide vanes passage, the components of frequency is similar to that of point 5. But the amplitude at every frequency decreases.

Point 8 is at the entrance of stay vanes passage. At this point, the frequency distribution has an obvious change. The first dominant frequency changes from $9f_n$ to $18f_n$. The second dominant frequency changes from $18f_n$ to $9f_n$. That means the runner influence becomes smaller and the vanes passages influence is getting more important. At the middle of the stay vanes passage, that is point 9, the amplitude decreases obviously. At the exit of the stay vanes passage (point 10), the fluctuation is at the lowest level. At the stay vanes passage, the other frequencies (except $4.5f_n$, $9f_n$, $18f_n$, and $27f_n$) have relatively high value. The four main frequencies have a low portion at the whole fluctuation energy, as shown in Figure 6. The amplitude change of those four frequencies is shown in Figure 7.

The horizontal axis in Figure 7 is the radius of the circle whose center is the center of the runner. When the radius is smaller than 300 mm, the first dominant frequency is $9f_n$, while when the radius is larger than that, the first dominant

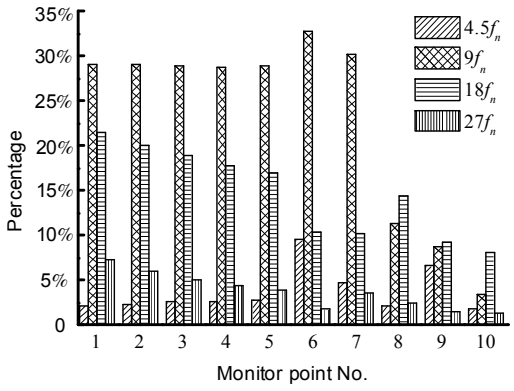

Figure 6 Portion of each frequency in mixing peak-to-peak values.

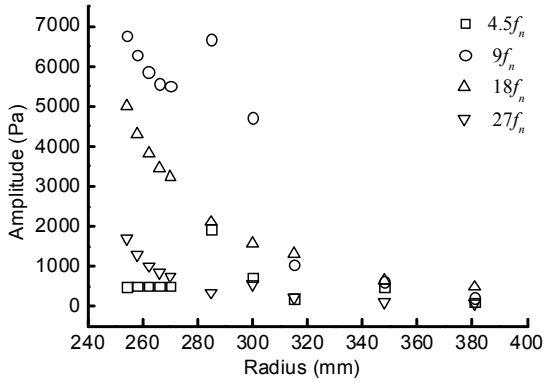

Figure 7 Change of amplitude of each frequency with the distance to runner center.

is $18f_n$. This has been analyzed before.

For $9f_n$, the highest amplitude appears at the nearest point to the runner, which is at a vaneless space. The amplitude decreases with the increase of the distance. However, at the guide vanes passage, the amplitude has an obvious leap. That may be induced by the interaction between the runner blades wake flow and the flow separation vortexes in the guide vanes passage. Nevertheless, the amplitude at this space is still smaller than the point nearest to the runner, which is at the vaneless space. Out of the guide vanes passage, the amplitude decreases with the increase of radius.

For $18f_n$ and $27f_n$, the changing curve is smooth. For $4.5f_n$ frequency component, the distribution law is different. Figure 7 shows that at the middle of the guide vanes passage, the pressure fluctuation has the peak value. Therefore, the source of this frequency should be at the guide vanes passage.

3.3 Pressure fluctuation propagation in the circumferential direction

As said before, five passages have been researched. The frequencies are different at each passage with the influence of the nonuniform flow distribution in the circumferential direction. The frequencies of different passages are shown in Figure 8.

Monitoring points 1–6 are located at the vaneless space and guide vanes passage. They are near the runner. All of the 20 guide vanes have the same structure and the same opening angle. Therefore, the frequency distributions are similar at these points in different passages. For the stay vanes passages, the situation is different from that in the guide vanes passages. There is a special stay vane. Its structure is different from the others. Therefore, the flow structure is asymmetrical around the circumferential direction. The influence of this special stay vane has been captured by the CFD method. In fact, at the exit of the guide vanes passage (point 7), this influence already has been observed. At the stay vanes area, the difference between

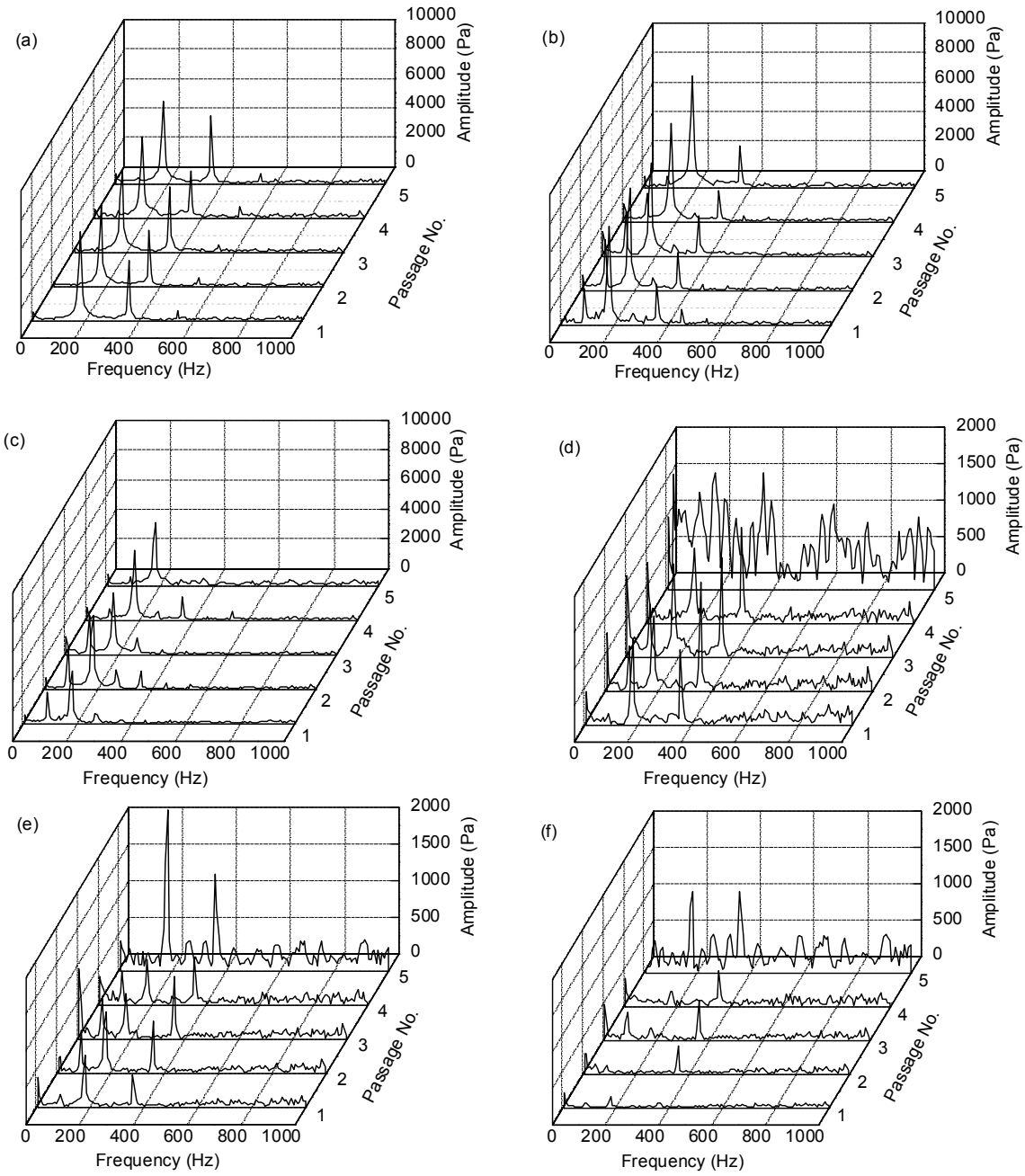

Figure 8 Frequency distribution of the different passages. (a) Monitoring point 5; (b) monitoring point 6; (c) monitoring point 7; (d) monitoring point 8; (e) monitoring point 9; (f) monitoring point 10.

each passage is clear. From passages 5 to 1, the amplitude decreases. As is shown in Figure 3, passages 5 and 1 are at the two sides of the special stay vane. In the pump mode, the pressure in passage 1 is high whereas the pressure in passage 5 is low.

4 Conclusion

The pressure fluctuation frequencies at the vaneless space and vanes passage are affected by the rotor-stator interaction. The amplitude of the pressure fluctuation decreases with the increase of the distance to runner. When the distance to runner center is smaller than 300 mm, the first dominant frequency is $9f_n$, which is the blades passing frequency. At the guide vanes passage, it has a steep rise. When the distance is larger than that, the first dominant frequency is $18f_n$. For $4.5f_n$, which is the semi-blades passing frequency, the peak value appears at the guide vanes passage. The first and second dominant frequency has a high portion in the mixed peak-to-peak value in the vaneless space and guide vanes passage, while in the stay vanes pas-

sage, this portion is low. The k-ω SST turbulence model has captured these propagation laws successfully.

The structural asymmetry of the stay vanes in the circumferential direction creates the nonuniform flow field and the fluctuations are different in different stay vanes passages. Pressure fluctuation in the low-pressure side passage of the special stay vane has the highest amplitude, while the passage of the other side of the special stay vane has the lowest amplitude.

This work was supported by the National Natural Science Foundation of China (Grant No. 51176168) and the National Key Technology Research and Development Program (Grant No. 2011BAF03B01).

1 Liu S H, Shao J, Wu S F, et al. Numerical simulation of pressure fluctuation in Kaplan turbine. Sci China Tech Sci, 2008, 51: 1137–1148
2 Husmatuchi V, Farhat M. Experiment investigation of a pump turbine at off design operating conditions. In: 3rd IAHR International meeting of the workgroup on cavitation and dynamic problems in hydraulic machinery and systems. Brno, Czech Republic, 2009. 339–347
3 Ran H J, Luo X W, Zhu L, et al. Experiment study of the pressure fluctuations in a pump turbine at large partial flow conditions. Sci China Tech Sci, 2012, 25: 1205–1209
4 Houde S, Fraser R, Ciocan G D, et al. Part 1-Experimental study of the pressure fluctuations on propeller turbine runner blades during steady-state operation. IOP Conf Series: Earth Environ Sci, 2012, 15: 022004
5 Yao Z F, Wang F J, Qu L X, et al. Experimental investigation of time-frequency characteristics of pressure fluctuations in a double-suction centrifugal pump. J Fluids Eng, 2011, 133: 101303
6 Chen T, Li S C. Numerical investigation of guide-plate induced pressure fluctuations on guide vanes of three gorges turbine. J Fluids Eng, 2011, 133: 061101
7 Xiao Y, Wang Z, Yan Z, et al. Experimental and numerical analysis of pressure pulses characteristics in a Francis turbine with partial load. IOP Conf Series: Earth Environ Sci, 2010, 12: 012023
8 Wang F J, Liao C L, Tang X L. Numerical simulation of pressure fluctuations in a large Francis turbine runner. Sci China Tech Sci, 2012, 25: 1198–1204
9 Gong R Z, Wang H G, Yao Y, et al. Numerical simulation of pressure fluctuation in 1000 MW Francis turbine under small opening condition. IOP Conf Series: Earth Environ Sci, 2012, 15: 062038
10 Qian Z D, Zheng B, Huai W X, et al. Analysis of pressure oscillations in a Francis hydraulic turbine with misaligned guide vanes. Proceedings of the institution of mechanical engineers, Part A: J Power Energy, 2010, 224: 139–152
11 Rivetti A, Lucinol C, Liscia S, et al. Pressure pulsation in Kaplan turbines: prototype-CFD comparison. IOP Conf Series: Earth Environ Scie, 2012, 15: 062035
12 Liu S H, Li S C, Wu Y L. Pressure fluctuation prediction of a model kaplan turbine by unsteady turbulent flow simulation. J Fluids Eng, 2009, 131: 101102
13 Wu Y L, Liu S H, Dou H S, et al. Numerical prediction and similarity study of pressure fluctuation in a prototype Kaplan turbine and the model turbine. Comput Fluids, 2012, 56: 128–142
14 Yang S S, Kong F Y, Qu X Y, et al. Influence of blade number on the performance and pressure pulsations in a pump used as a turbine. J Fluids Eng, 2012, 134: 124503
15 Zobeiri A, Kueny J L, Avellan F. Pump-turbine rotor-stator interactions in generating mode: Pressure fluctuation in distributor channel. In: 23rd IAHR symposium on hydraulic machinery and systems, Yokohama, Japan, 2006
16 Xiao Y X, Sun D G, Wang Z W, et al. Numerical analysis of unsteady flow behavior and pressure pulsation in pump turbine with misaligned guide vanes. IOP Conf Series: Earth Environ Sci, 2012, 15: 032043
17 Liu J T, Liu S H, Sun Y K, et al. Numerical simulation of pressure fluctuation of a pump turbine with MGV at no-load condition. IOP Conf Series: Earth Environ Sci, 2012, 15: 062036
18 Sun H, Xiao R F, Liu W C, et al. Analysis of S characteristics and pressure pulsations in a pump-turbine with Misaligned guide vanes. J Fluids Eng, 2013, 135: 051101
19 Sun Y K, Zuo Z G, Liu S H, et al. Numerical study of pressure fluctuations in different guide vanes' opening angle in pump mode of a pump turbine. IOP Conf Series: Earth Environ Scie, 2012, 15: 062037
20 Spence R, Joao A T. Investigation into pressure pulsation in a centrifugal pump using numerical methods supported by industrial test. Comput Fluids, 2008, 37: 690–704
21 Shi F, Tsukamoto H. Numerical study of pressure fluctuations caused by impeller-diffuser interaction in a diffuser pump stage. J Fluids Eng, 2001, 123: 466–474
22 Wang H, Tsukamoto H. Experimental and numerical study of unsteady flow in a diffuser pump at off-design conditions. J Fluids Eng, 2003, 125: 767–778
23 Menter F R. Two-equation eddy-viscosity turbulence models for engineering applications. AIAA J, 1994, 32: 1598–1605